



Enhanced Magneto-Optical Edge Excitation in Nanoscale Magnetic Disks

A. Berger,¹ R. Alcaraz de la Osa,² A. K. Suszka,^{1,*} M. Pancaldi,¹ J. M. Saiz,² F. Moreno,² H. P. Oepen,³ and P. Vavassori^{1,4}

¹*CIC nanoGUNE, E-20018 Donostia-San Sebastian, Spain*

²*Grupo de Óptica. Departamento de Física Aplicada. Universidad de Cantabria, Avenida de los Castros s/n, Santander, Spain*

³*Institut für Angewandte Physik, Universität Hamburg, Jungiusstraße 11, 20355 Hamburg, Germany*

⁴*IKERBASQUE, Basque Foundation for Science, 48011 Bilbao, Spain*

(Received 30 October 2014; revised manuscript received 25 June 2015; published 30 October 2015)

We report unexpected enhancements of the magneto-optical effect in ferromagnetic Permalloy disks of diameter $D < 400$ nm. The effect becomes increasingly pronounced for smaller D , reaching more than a 100% enhancement for $D = 100$ nm samples. By means of experiments and simulations, the origin of this effect is identified as a nanoscale ring-shaped region at the disk edges, in which the magneto-optically induced electric polarization is enhanced. This leads to a modification of the electromagnetic near fields and causes the enhanced magneto-optical excitation, independent from any optical resonance.

DOI: 10.1103/PhysRevLett.115.187403

PACS numbers: 78.20.Ls, 78.20.Jq, 78.67.Bf, 78.68.+m

Nanophotonics has become a burgeoning field of research based upon the formidable ability of metallic nanostructures to strongly localize and enhance electromagnetic fields [1–3]. This has led to unprecedented control of intensity and polarization of light, which has also been exploited in a broad range of applications, such as novel nano-optical devices for communications [4], energy harvesting [5], biosensors [6–10], and photonic crystal structures [11]. The vast majority of studies in this field has been performed on nonmagnetic metallic nanostructures and focused primarily on localized surface plasmon resonances [12]. Nanostructures using magneto-optically active materials, such as metallic ferromagnets, started to attract attention only recently, leading to the rapidly developing field of magnetoplasmonics, which combines concepts of plasmonics and magnetism for the purpose of unveiling novel phenomena and functionalities at the nanoscale [13–24]. Key findings are hereby the ability to magnetically influence plasmonic properties and in return influence magneto-optical effects via plasmon resonances. Despite this large interest in nanoscale magneto-optics, only a few works have investigated the relevant fundamental effects arising from the interplay between magneto-optical activity and light-matter coupling in spatially confined geometries that are independent from resonance excitations [25–27]. In addition to, and in conjunction with magnetoplasmonics, such effects could lead to novel functionalities for the manipulation of light at the nanoscale, which are expected to play a major role in the emerging technology of flat optics [28,29].

To elucidate the physics of magneto-optical activity in nanoscale confined geometries and to investigate associated modifications of magneto-optical signals, we have studied here the size dependent magneto-optical response for nanoscale disks. We investigate this subject by means of experiments based upon magneto-optical diffraction

measurements as well as simulations utilizing the extended discrete dipole approximation (E-DDA) [26]. Details of this theoretical approach, including the incorporation of magneto-optical activity by means of a nondiagonal dielectric tensor

$$\vec{\epsilon} = \begin{pmatrix} \epsilon_d & -i\epsilon_d Q & 0 \\ i\epsilon_d Q & \epsilon_d & 0 \\ 0 & 0 & \epsilon_d \end{pmatrix} \quad (1)$$

have been described previously [27]. Hereby, ϵ_d is the conventional dielectric function, Q is the magneto-optical coupling constant, and matching our experimental conditions, the tensor in Eq. (1) assumes a z -axis orientation of the magnetization (see Fig. 1).

As shown in Fig. 1, our samples consist of two-dimensional rectangular arrays of Permalloy disks that were fabricated using electron beam lithography. The disk diameter D was varied from 100 to 800 nm, and the rectangular lattice periods set to $a = D + 200$ nm and $b = 1.8 \mu\text{m}$. Period b was chosen to be sufficiently large, so that the reflected light produced several diffraction orders. Also, it was held constant to enable the observation of the diffracted light under identical angular conditions for all samples, which allows for a direct quantitative comparison of our results [30]. Period a was made smaller to have a sufficiently high surface area covered by the magnetic material. By keeping the interdisk spacing constant at 200 nm, which corresponds to at least 8 times the disk thickness, we are also avoiding possible complications caused by significant optical coupling in between the disks, which is corroborated by simulations of the magneto-optical effects investigated here [30]. The calculations verify that disk interactions cause modifications of only about 2% in the magneto-optical effects, even for large disks of the maximum thickness used in our experiment

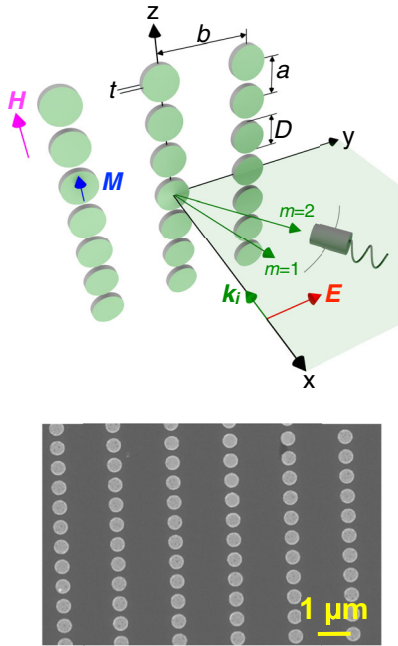


FIG. 1 (color online). Schematic of sample and measurement geometry: disks of diameter D and thickness t are arranged in a parallel line array with an interline spacing of $b = 1.8 \mu\text{m}$, so that the incoming light produces clearly visible diffraction. Diffraction orders $m = 1$ and $m = 2$ are indicated here for the normal incidence case ($k_i \parallel x$ - axis). The incoming light is linearly polarized along the y direction, while the externally applied magnetic field H is aligned along the z axis. The inset shows a SEM picture of the $D = 400 \text{ nm}$ experimental sample, fabricated by means of electron beam lithography.

[30]. Figure 1 also shows a scanning electron microscopy (SEM) picture of one of our samples and defines our magneto-optical observation geometry. In our experiments, linearly polarized laser light of wavelengths $\lambda = 532 \text{ nm}$ and $\lambda = 633 \text{ nm}$ was used in normal incidence geometry with the electric polarization aligned within the diffraction plane (xy plane). A magnetic field H was applied perpendicular to the diffraction plane, and the H dependence of the light intensity in diffraction orders $m = 1$ and $m = 2$ was measured. This specific geometry allows the observation of magneto-optical effects as simple intensity changes, which makes it robust against topography induced polarization changes of the diffracted light, which can vary from sample to sample.

Figure 2 shows examples of magnetic hysteresis loops measured as relative diffracted light intensity change $\Delta I/I$ as a function of H , with I being the light intensity and ΔI being the magnetic field induced change in I . Specifically, Fig. 2(a) displays measurements for $m = 1$ with $\lambda = 532 \text{ nm}$ for disks of different D and thickness $t = 25 \text{ nm}$, while Fig. 2(b) shows the corresponding signals for $\lambda = 633 \text{ nm}$. The *pinched* shape of the loops is very typical for nanodisks due to the occurrence of low field vortex states, in which the magnetization describes a circular

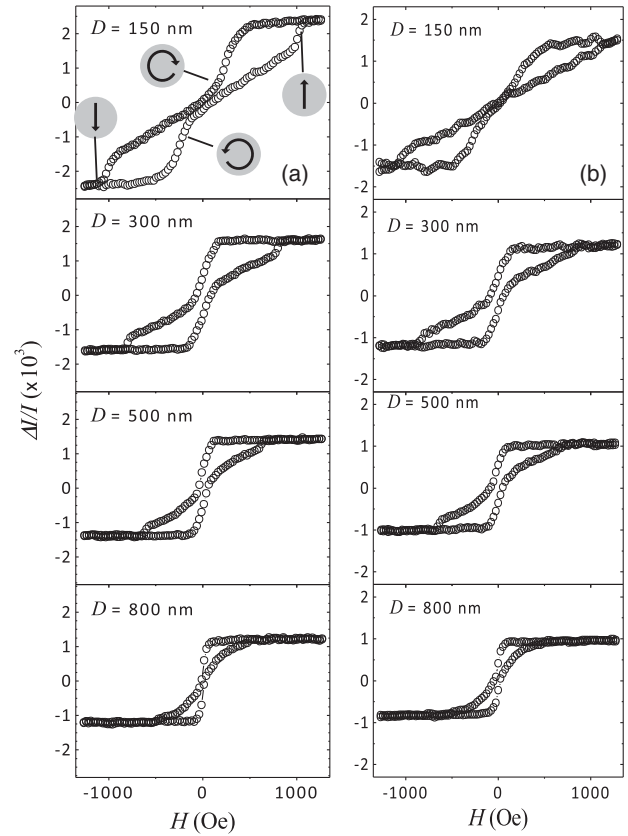


FIG. 2. Transverse magneto-optical signal $\Delta I/I$ vs applied magnetic field strength H for samples of different diameter D , measured for light of wavelength (a) $\lambda = 532 \text{ nm}$ and (b) $\lambda = 633 \text{ nm}$. The insets in the topmost figure of (a) are schematic representations of the magnetization states at different field values following a complete hysteresis loop cycle. The measurements shown here were acquired for $m = 1$ and a sample with $t = 25 \text{ nm}$.

pattern [31]. Upon lowering H , the disk magnetization proceeds from a uniform “up” state to the vortex state, and then to the magnetic “down” state for large negative fields. Upon increasing the field again, the sequence is reversed as indicated by the cartoons in Fig. 2(a). The transformation of the “up” or “down” states into the vortex state requires thermal activation, which causes a magnetic hysteresis phenomenon. The hysteresis becomes less important for larger disks, which is consistent with the activation barrier behavior reported in the literature [31]. Figure 2 also demonstrates that measurements for the different λ show consistent results, as do the data for $m = 2$, which are shown in the Supplemental Material [30]. Also, we find that the signals at high magnetic fields are field independent, because the magnetic material is saturated already. Furthermore, no relevant background signal is observed. Thus, we can equate our high-field measured $\Delta I/I$ values as being produced by the inversion of a uniform magnetization state along the z direction of the disk.

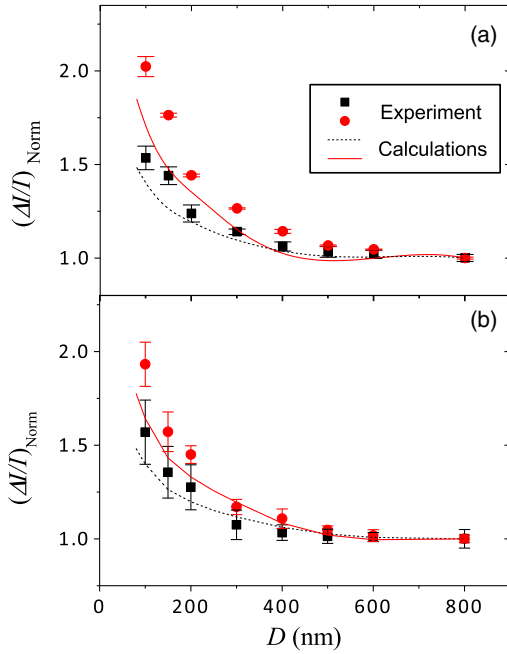


FIG. 3 (color online). Normalized transverse magneto-optical signal $\Delta I/I$ in saturation vs disk diameter D for light of wavelength (a) $\lambda = 532$ nm and (b) $\lambda = 633$ nm. The experimental data for 15 nm and 25 nm thick disks are shown as (black) squares and (red) dots, respectively. The lines represent results derived from E-DDA calculations using the exact same geometry as the experiment. All data are normalized to their respective values at $D = 800$ nm.

We also notice in Fig. 2 that the total signal level $\Delta I/I$ is larger for smaller D for both wavelengths. This is an unexpected result, because the magnetic material and thus the magneto-optical coupling strength is identical in all samples and should produce a Kerr effect of constant strength [27]. To study this anomalous enhancement, the absolute Kerr effect $\Delta I/I$ for samples of varying D and t was measured. The results are shown in Fig. 3, where the Kerr effect at the maximum applied field strength $H = 1200$ Oe is plotted to insure that we are always in the saturated magnetization state. In all cases, i.e., for different t and λ , an enhancement of the magneto-optical signal is observed upon reducing D . Hereby, the signal increase is not a small perturbation, but instead an about 100% enhancement effect for the $D = 100$ nm disks over the $D = 800$ nm sample. Also, we find that the enhancement is larger for thicker disks, while the specific wavelength λ has very little influence. Together with the experimental observation that our samples do not exhibit a plasmon resonance in the here studied spectral range [30], this wavelength independence indicates that plasmonic resonances are not relevant for the here observed enhancement effect. Also, we find the enhancement to be independent from the diffraction order [30]. Thus, it cannot be caused by an observation specific interference effect, but must be due to the electric field and polarization pattern in the disks. To elucidate the

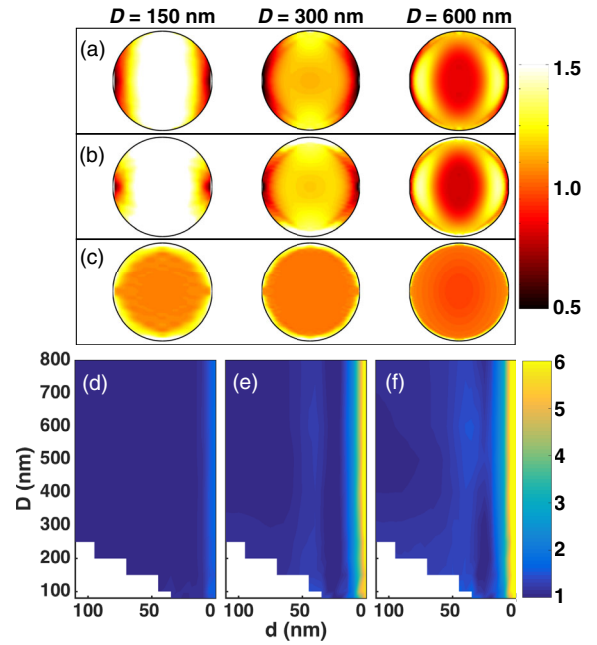


FIG. 4 (color online). (a)–(c) show the lateral distribution of the (a) primary optical (P_y) and (b) magneto-optical (P_x) components of the induced dipole moment, as well as (c) their ratio P_x/P_y for nanoscale disks of size D and $t = 5$ nm. The gray (color) scale is normalized to the corresponding values of an infinite film of equal thickness. Plots (d), (e), and (f) show normalized (to the infinite film calculation) P_x/P_y -ratio maps as a function of the distance to the disk edge d and the disk diameter D for $t = 5$ nm (d), 15 nm (e), and 25 nm (f), respectively. The corresponding gray (color) scale that is shown on the right-hand side of (f) applies also to (d) and (e).

origin of this magneto-optical enhancement effect, we performed E-DDA calculations for our experimental geometry. Given that disk interactions can be neglected [30], we have first calculated the fully self-consistent response of an individual disk of given size, and then placed replicas of the solution onto each lattice site to calculate the far-field signals.

For the dielectric tensor of bulk Permalloy, literature values were used [32]. The theoretically predicted $\Delta I/I$ vs D dependence is also shown in Fig. 3 in direct comparison to the experimental data. Our calculations show exactly the same trends as the experiments regarding the disk diameter D , the disk thickness t , and wavelengths λ . Only for very small disks, namely $D < 200$ nm, there is a visible difference between the experimental data and the simulated results. Here, the experimental enhancement is even larger than what our calculations predict. However, overall, the model calculations are in excellent agreement with our experiments.

To understand the origin of the enhancement effect, the lateral distribution of the electric field induced polarization P is plotted in Figs. 4(a)–4(c) for three different disk diameters D . Figure 4(a) shows the y -axis polarization P_y ,

which is parallel to the electric field of the incoming light wave and thus, the largest polarization component that builds up upon excitation. Furthermore, our geometry leads to a coupling of the x - y components of the electric field and polarization, as described by the dielectric tensor in Eq. (1). Thus, the resulting P_x and P_y pattern describe the relevance of the magneto-optical response in the light excitation process, and the observed magneto-optical intensity effect stems from the phase sensitive far-field radiation superposition of both components. Without magneto-optical coupling, no sample-averaged P_x polarization would occur in our disks. Figure 4(b) displays the magneto-optically induced polarization P_x , while Fig. 4(c) shows the local distribution of the ratio P_x/P_y . In each case, the quantity is normalized to the respective values that occur in an infinite film of the same thickness and material.

Figures 4(a) and 4(b) show that the optical and magneto-optical excitations are nonuniform. This, of course, is the net effect of the sample shape and the corresponding electromagnetic boundary conditions at the disk surfaces. Upon visually comparing the P_y and P_x maps for each size, we see that both are nearly identical, because their behavior is dominated by the local electric field in the y direction E_y . This field component is laterally varying, but it drives optical and magneto-optical responses in virtually the same way according to Eq. (1), because magneto-optical modifications are typically only a small perturbation [27]. However, if this were the complete physical picture, the relative strength of the magneto-optical response would be given by the size of the off diagonal element in the dielectric tensor alone and thus not dependent on the size of the disks. Therefore, it cannot explain the observed enhancement.

The origin of the size-dependent enhancement of the Kerr effect becomes apparent from the P_x/P_y -ratio maps in Fig. 4(c). Here, the center portions of the disks display a magneto-optical response ratio that matches the infinite film case. However, one can also see a bright ringlike structure at the disk edges, for which the relative magneto-optical response is substantially larger. It is this P_x/P_y enhancement ring that is responsible for the signal increase. We have corroborated this fact by comparing our results here with the quasiscalar approximation [27], in which the disk polarization pattern is first calculated by assuming a diagonal dielectric tensor and subsequently, the magneto-optical response is computed by locally applying Eq. (1). The so-computed P_x and P_y pattern are almost identical to the ones shown in Fig. 4 with the only difference being the disappearance of the P_x/P_y enhancement ring. In this quasiscalar approximation, $\Delta I/I$ does not exhibit any D dependent enhancement, because the shape induced confinement effects onto P_x that lead to the ring-shaped enhancement of P_x are excluded.

The ring enhancement actually occurs in a nearly identical way for disks of all sizes. This can be seen in Figs. 4(d), 4(e), and 4(f), where we have plotted P_x/P_y -ratio maps as a function of the distance to the edge d and the diameter D for three different values of t . The P_x/P_y edge enhancement produces a bandlike feature on the right-hand side in each plot, because it is essentially independent from D . This means that for a constant t , the enhancement ring has the same absolute width for all D . Thus, it is simply the relative geometric size of the ring area in comparison to the total disk area that increases with decreasing D . The comparison of Figs. 4(d)–4(f) also shows that ring size and P_x/P_y ratios increase with t , at least for sufficiently small t . As a consequence, the Kerr effect enhancement is larger for thicker disks, which is exactly what we find in our experiment. The P_x/P_y enhancement profiles are primarily determined by the disk geometry due to a radially dependent depolarization effect near the edges [30], which changes with thickness. The finite light penetration depth caused by optical absorption now limits the effective disk surface region that contributes to the edge enhancement effect. This in turn leads to a saturation of the thickness dependence for the observable P_x/P_y enhancement and its associated ring width, which is less than 15 nm for bulk Permalloy in the wavelength range explored here [30]. This edge localization can also explain why the experimental enhancement is visibly larger than theoretically predicted for very small D . Any deviation from a perfect circular shape in real samples will lead to an edge length increase, which can cause a further enhancement of the magneto-optical effect. Given that the edge region area of a disk corresponds to a larger fraction of the total disk area for smaller disks, such imperfection enhancements will be most visible for the smallest disks [30].

In summary, we observe an unexpected enhancement of the magneto-optical effect for Permalloy disks with a diameter $D < 400$ nm. The effect becomes increasingly pronounced for smaller D , reaching more than a 100% enhancement for $D = 100$ nm samples. By means of simulations, we are able to reproduce the experimental behavior, including its dependence on D , disk thickness t , wavelengths λ , and diffraction order m . The simulations furthermore identify the origin of this effect as a ring-shaped region at the disk edges, where the magneto-optically induced electric polarization is enhanced. This leads to an enhancement of the magneto-optical effect, independent from any optical resonance. The edge-induced enhancement effect is substantial, even if the absolute size of the magneto-optical effect in our samples remains modest. However, far larger absolute values should be achievable by utilizing materials with substantially larger magneto-optical coupling strengths Q and even smaller nanoscale dimensions or substructures.

We acknowledge funding from the Basque Government (Program No. PI2012-47) and the Spanish Government (Project No. MAT2012-36844). Work at the Universidad de Cantabria has been supported by MICINN under Project No. FIS2013-45854-P.

*Present address: Laboratory for Mesoscopic Systems, Department of Materials, ETH Zurich, 8093 Zurich, Switzerland, Laboratory for Micro- and Nanotechnology, Paul Scherrer Institute, 5232 Villigen PSI, Switzerland.

- [1] L. Novotny and N. van Hulst, *Nat. Photonics* **5**, 83 (2011).
- [2] M. I. Stockman, *Phys. Today* **64**, 39 (2011).
- [3] V. Giannini, A. I. Fernandez-Dominguez, S. C. Heck, and S. A. Maier, *Chem. Rev.* **111**, 3888 (2011).
- [4] M. Sandtke and L. Kuipers, *Nat. Photonics* **1**, 573 (2007).
- [5] V. E. Ferry, L. A. Sweatlock, D. Pacifici, and H. A. Atwater, *Nano Lett.* **8**, 4391 (2008).
- [6] T. Chung, S. Y. Lee, E. Y. Song, H. Chun, and B. Lee, *Sensors* **11**, 10907 (2011).
- [7] K. M. Mayer and J. H. Hafner, *Chem. Rev.* **111**, 3828 (2011).
- [8] E. M. Larsson, S. Syrenova, and C. Langhammer, *Nanophotonics* **1**, 249 (2012).
- [9] V. G. Kravets *et al.*, *Nat. Mater.* **12**, 304 (2013).
- [10] S. S. Aćimović, M. A. Ortega, V. Sanz, J. Berthelot, J. L. Garcia-Cordero, J. Renger, S. J. Maerkl, M. P. Kreuzer, and R. Quidant, *Nano Lett.* **14**, 2636 (2014).
- [11] T. Baba, *Nat. Photonics* **2**, 465 (2008).
- [12] See, e.g., M. I. Stockman, *Opt. Express* **19**, 22029 (2011), and references therein.
- [13] J. B. González-Díaz, A. García-Martín, J. M. García-Martín, A. Cebollada, G. Armelles, B. Sepúlveda, Y. Alaverdyan, and M. Käll, *Small* **4**, 202 (2008).
- [14] Z. Liu, L. Shi, Z. Shi, X. H. Liu, J. Zi, S. M. Zhou, S. J. Wei, J. Li, X. Zhang, and Y. J. Xia, *Appl. Phys. Lett.* **95**, 032502 (2009).
- [15] V. V. Temnov, G. Armelles, U. Woggon, D. Guzatov, A. Cebollada, A. García-Martín, J. M. García-Martín, T. Thomay, A. Leitenstorfer, and R. Bratschitsch, *Nat. Photonics* **4**, 107 (2010).
- [16] V. I. Belotelov, I. A. Akimov, M. Pohl, V. A. Kotov, S. Kasture, A. S. Vengurlekar, A. V. Gopal, D. R. Yakovlev, A. K. Zvezdin, and M. Bayer, *Nat. Nanotechnol.* **6**, 370 (2011).
- [17] J. Chen *et al.*, *Small* **7**, 2341 (2011).
- [18] V. Bonanni, S. Bonetti, T. Pakizeh, Z. Pirzadeh, J. Chen, J. Nogués, P. Vavassori, R. Hillenbrand, J. Åkerman, and A. Dmitriev, *Nano Lett.* **11**, 5333 (2011).
- [19] J. C. Bantón, D. Meneses-Rodríguez, F. García, M. U. González, A. García-Martín, A. Cebollada, and G. Armelles, *Adv. Mater.* **24**, OP36 (2012).
- [20] V. V. Temnov, *Nat. Photonics* **6**, 728 (2012).
- [21] V. I. Belotelov *et al.*, *Nat. Commun.* **4**, 2128 (2013).
- [22] J. Y. Chin, T. Steinle, T. Wehler, D. Dregely, T. Weiss, V. I. Belotelov, B. Stritzker, and H. Giessen, *Nat. Commun.* **4**, 1599 (2013).
- [23] G. Armelles, A. Cebollada, A. García-Martín, and M. U. González, *Adv. Opt. Mater.* **1**, 10 (2013).
- [24] N. Maccaferri *et al.*, *Phys. Rev. Lett.* **111**, 167401 (2013).
- [25] S. Albaladejo, R. Gómez-Medina, L. S. Froufe-Pérez, H. Marinchio, R. Carminati, J. F. Torrado, G. Armelles, A. García-Martín, and J. J. Sáenz, *Opt. Express* **18**, 3556 (2010).
- [26] R. Alcaraz de la Osa, P. Albella, J. M. Saiz, F. Gonzalez, and F. Moreno, *Opt. Express* **18**, 23865 (2010).
- [27] R. Alcaraz de la Osa, J. M. Saiz, F. Moreno, P. Vavassori, and A. Berger, *Phys. Rev. B* **85**, 064414 (2012).
- [28] N. Yu and F. Capasso, *Nat. Mater.* **13**, 139 (2014).
- [29] A. V. Kildishev, A. Boltasseva, and V. M. Shalaev, *Science* **339**, 1232009 (2013).
- [30] See Supplemental Material at <http://link.aps.org/supplemental/10.1103/PhysRevLett.115.187403> for a description of further details related to Transverse Magneto-optical Kerr effect observation in diffraction, the spectral response of our samples, the role of disk-to-disk interactions, the lateral size of the enhancement ring, and a visualization of fabrication limits.
- [31] M. Grimsditch and P. Vavassori, *J. Phys. Condens. Matter* **16**, R275 (2004).
- [32] Optical and MO constants were taken from G. S. Krinchik and V. A. Artem'ev, *Sov. Phys. JETP* **26**, 1080 (1968); and an effective dielectric tensor using the Maxwell-Garnett formalism was obtained, as described in R. Alcaraz de la Osa, F. Moreno, and J. M. Saiz, *Opt. Commun.* **291**, 405 (2013).